

METHODS & TECHNIQUES

A novel technique for the precise measurement of CO₂ production rate in small aquatic organisms as validated on aeshnid dragonfly nymphs

Till S. Harter*, Colin J. Brauner and Philip G. D. Matthews

ABSTRACT

The present study describes and validates a novel yet simple system for simultaneous *in vivo* measurements of rates of aquatic CO₂ production (\dot{M}_{CO_2}) and oxygen consumption (\dot{M}_{O_2}), thus allowing the calculation of respiratory exchange ratios (RER). Diffusion of CO₂ from the aquatic phase into a gas phase, across a hollow fibre membrane, enabled aquatic \dot{M}_{CO_2} measurements with a high-precision infrared gas CO₂ analyser. \dot{M}_{O_2} was measured with a P_{O₂} optode using a stop-flow approach. Injections of known amounts of CO₂ into the apparatus yielded accurate and highly reproducible measurements of CO₂ content ($R^2=0.997$, $P<0.001$). The viability of *in vivo* measurements was demonstrated on aquatic dragonfly nymphs (Aeshnidae; wet mass 2.17 mg–1.46 g, $n=15$) and the apparatus produced precise \dot{M}_{CO_2} ($R^2=0.967$, $P<0.001$) and \dot{M}_{O_2} ($R^2=0.957$, $P<0.001$) measurements; average RER was 0.73 ± 0.06 . The described system is scalable, offering great potential for the study of a wide range of aquatic species, including fish.

KEY WORDS: Stop-flow, Hypoxia, Respirometer, Validation, Fish, Insect, Respiratory quotient

INTRODUCTION

The development of high-precision non-dispersive infrared CO₂ analysers has made available a powerful tool for the measurement of CO₂ production rates (\dot{M}_{CO_2}) in air-breathers, but overlapping absorption spectra of CO₂ and H₂O preclude their use in aqueous media. However, it is possible to promote diffusion of CO₂ from the water to a gas phase that can then be analysed with infrared analysers, a principle that has been used for discontinuous measurements of dissolved CO₂ in aquaculture (Pfeiffer et al., 2011; Stiller et al., 2013), but relying entirely on the equilibration of water CO₂ with an air-filled head space.

The present study describes a simple aquatic respirometer for simultaneous *in vivo* measurements of \dot{M}_{CO_2} and oxygen consumption rate (\dot{M}_{O_2}) in small aquatic organisms. The novel aspect of this apparatus is the use of a hollow fibre membrane (HFM) as the interface between aquatic and gas phases, providing a large ratio of gas exchange surface area to system volume. Similar HFM designs are finding increasing application as oxygenators in human medicine (Nolan et al., 2011; Potkay, 2014; Strueber, 2015). The high precision, and thus suitability, of the apparatus for

measuring small aquatic \dot{M}_{CO_2} was validated both *in vitro* and *in vivo* using aeshnid dragonfly nymphs.

MATERIALS AND METHODS

Animal collection and husbandry

Aeshnid dragonfly nymphs (*Aeshna* spp. and *Anax junius*; wet mass 2.17 mg–1.46 g; $n=15$) were caught in the experimental ponds at the University of British Columbia (summer 2016), and were held in the laboratory for several weeks before experiments. Housing was in 1 l glass containers connected to a recirculation system supplied with dechlorinated Vancouver tap water at room temperature (22°C). Animals were fed various wild-caught aquatic insects, twice a week.

Experimental setup

The central component of the apparatus for the measurement of \dot{M}_{CO_2} and \dot{M}_{O_2} was a HFM that created a high surface-area interface between counter-current flows of water and CO₂-free air (Fig. 1). CO₂ added to the water phase rapidly diffused down its partial pressure gradient, across the HFM and into the gas phase, where it was measured with a LI-7000 differential CO₂ analyser (LiCor, Lincoln, NE, USA).

The HFM consisted of 34 lengths of Oxyplus polymethylpentene fibres (Membrana, Wuppertal, Germany; diameter=380 µm, length=100 mm, area=4059 mm²; see Fig. S5) arranged in parallel and fitted into a 1/8 inch acrylic tube, similar to previous designs (Kaar et al., 2007; Arazawa et al., 2012). The volume surrounding the fibres (0.6 ml) was perfused with water coming from the measuring chamber that was circulated in a closed loop by a peristaltic pump (Gilson MINIPULS 3, Middleton, WI, USA). The lumen of the fibres (0.4 ml volume) was perfused with CO₂-free air, produced in a CDA4-CO₂ purge-gas generator (Puregas, Broomfield, CO, USA) and passed through columns of Drierite (Hammond Drierite, Xenia, OH, USA) and soda lime (Spectrum Chemical, New Brunswick, NJ, USA). Air flow rates were set to either 20 or 50 ml min⁻¹ (depending on the magnitude of the CO₂ signal) with MC Standard Series mass-flow controllers (Alicat Scientific, Tucson, AZ, USA).

CO₂-free air was water-saturated in a sparging column and passed through the HFM, where it took up CO₂ from the water. Thereafter, the air was de-humidified in 25 cm of TT-070 Nafion tubing (Permapure, Lakewood, NJ, USA), housed in a chamber flushed with dry air at 600 ml min⁻¹ (residual water content during analysis was <1 mmol mol⁻¹). Air containing CO₂ from the water was passed through channel B of the CO₂ analyser and a separate stream of dry CO₂-free purge-gas was passed through channel A. Channels A and B were subtracted from one another, providing an internal control for variability in purge-gas composition. The CO₂ analyser was calibrated using analytical grade N₂ and 1000 ppm CO₂ in N₂, and the calibration was confirmed periodically. Gas flow rates

Department of Zoology, University of British Columbia, 6270 University Boulevard, Vancouver, BC, Canada V6T 1Z4.

*Author for correspondence (harter@zoology.ubc.ca)

 T.S.H., 0000-0003-1712-1370

List of symbols and abbreviations

[CO ₂]	concentration of CO ₂
<i>f</i>	flow rate
HFM	hollow fibre membrane
<i>m</i>	mass
<i>P</i>	pressure
<i>P</i> _{O₂}	partial pressure of O ₂
RER	respiratory exchange ratio
STP	standard temperature and pressure
<i>t</i>	time
<i>V</i>	volume
\dot{M}_{CO_2}	CO ₂ production rate
\dot{M}_{O_2}	O ₂ consumption rate
α_{CO_2}	solubility of CO ₂ in water
α_{O_2}	solubility of O ₂ in water

through the CO₂ analyser were measured at the outlet with a DryCal Definer 220 positive displacement volumetric flow meter (MesaLabs, Butler, NJ, USA); these values were used for calculations.

The measuring chambers consisted of glass scintillation vials (1.9, 4.7 or 24.5 ml volume) fitted with ports for water inlets and outlets and a *P*_{O₂} (partial pressure of O₂) optode with MicroxTX3 meter (Loligo Systems, Viborg, Denmark); optodes were calibrated before each trial using a sodium sulfite solution and air-equilibrated dH₂O. A PVC mesh was fitted inside the vials to provide a resting structure for the nymph, and mixing was with a magnetic stir bar that was covered by an aluminium grid to protect the animal (Fig. S5). Water flow rates replaced the vial volume every minute for the smaller vials and every 2 min for the largest vial (i.e. 1.9, 4.7, 12.3 ml min⁻¹). Water pH was measured with a flow-through pH microelectrode (Microelectrodes Inc., Bedford, NH, USA) after the measuring chamber, which was calibrated before each run with BDH precision buffers (VWR, Radnor, PA, USA).

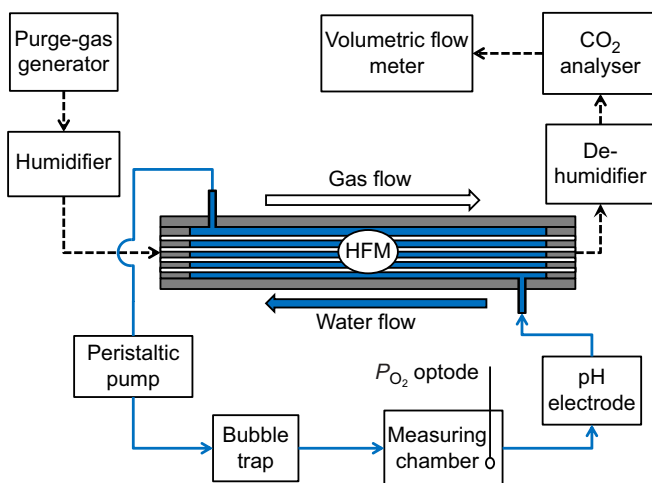


Fig. 1. Schematic representation of the experimental apparatus for the measurement of rates of CO₂ production (\dot{M}_{CO_2}) and O₂ consumption (\dot{M}_{O_2}) in small aquatic organisms. Water was circulated in a closed loop indicated by the blue arrows, and CO₂-free purge-gas is represented by the dashed arrows. The interface between water and air was a hollow fibre membrane (HFM) gas exchanger, in which water was circulated on the outside of a bundle of gas permeable fibres and CO₂-free purge-gas was circulated through the lumen of the fibres in a counter-current fashion, similar to previous designs (Kaar et al., 2007; Arazawa et al., 2012). See Materials and methods, Experimental setup for specifications of system components.

Experimental design

Before each trial, the system was flushed and filled with CO₂-free, dechlorinated Vancouver tap water, which was generated in a glass vessel that was continuously sparged with CO₂-free air from the purge-gas generator at 600 ml min⁻¹. All experiments were carried out at room temperature (22°C).

In Series 1, the experimental setup was validated by injecting known amounts of CO₂-saturated dH₂O into the measuring chamber and recording the corresponding peaks in CO₂ concentration ([CO₂]) in the gas phase. CO₂-saturated water was generated by sparging a column (height=0.35 m) of dH₂O with 100% CO₂. To ensure complete recovery of injected CO₂ through the analyser, water in the system was acidified by addition of 10% (v/v) 0.01 mol l⁻¹ HCl (average water pH was 3.6±0.1). After each set of four CO₂ injections (5, 10, 15 and 20 µl), the water in the system was replaced, and six replicate runs were performed (*n*=6).

In Series 2, the experimental setup was validated for the measurement of \dot{M}_{CO_2} (and \dot{M}_{O_2}) in dragonfly nymphs. The system was flushed and filled with CO₂-free water and a baseline measurement was performed without an animal (phase i). Thereafter, a nymph was introduced into the measuring chamber, which was then covered to minimise disturbance. Once stable readings were obtained (phase ii) the peristaltic pump was stopped, and the decline in water *P*_{O₂} was recorded for the calculation of \dot{M}_{O_2} (phase iii). When *P*_{O₂} had decreased to 100 mmHg, water flow was re-started and the accumulated CO₂ was washed out of the system, resulting in a peak in [CO₂] measured in the gas phase (phase iv). After this washout period, a second set of animal recordings was performed (phase v). Immediately after the trial, the nymph was blotted dry and weighed on an XPE205 electronic balance (Mettler Toledo, Columbus, OH, USA).

Calculations and data analysis

All parameters were recorded continuously with a PowerLab data acquisition unit (ADInstruments, Dunedin, New Zealand) and raw data were analysed with Labchart v8.1.5.

In Series 1, the content of CO₂ in the injected water was calculated as:

$$\text{CO}_2 \text{ injected} = \alpha_{\text{CO}_2} \times P \times \frac{V}{1000}, \quad (1)$$

where α_{CO_2} (mmol l⁻¹ mm Hg⁻¹) is the solubility of CO₂ in water (Boutilier et al., 1984); *P* is total gas pressure, calculated from atmospheric pressure (average 762±2 mmHg), the height of the sparging column (0.35 m) and subtracting the water vapour pressure (Dean, 1999); and *V* is the injected volume of CO₂-saturated water.

The content of CO₂ measured with the CO₂ analyser was calculated as:

$$\text{CO}_2 \text{ measured} = \frac{\int_{t_1}^{t_2} [\text{CO}_2] \times f \times 1000}{V}, \quad (2)$$

where [CO₂] is the concentration of CO₂ (ppm), *f* is the gas flow rate (ml min⁻¹; STP) and *V* is the volume of CO₂ gas (22.4 l mol⁻¹; STP). The integral under the [CO₂] curve was calculated from the time of injection (*t*₁) until [CO₂] returned to baseline (*t*₂) (see Fig. 2B).

In Series 2, continuous \dot{M}_{CO_2} was calculated from the animal recording of [CO₂] before (phase ii) and after the stop-flow period (phase v) and subtracting the baseline reading without the animal (phase i). \dot{M}_{CO_2} during stop-flow was calculated as described in

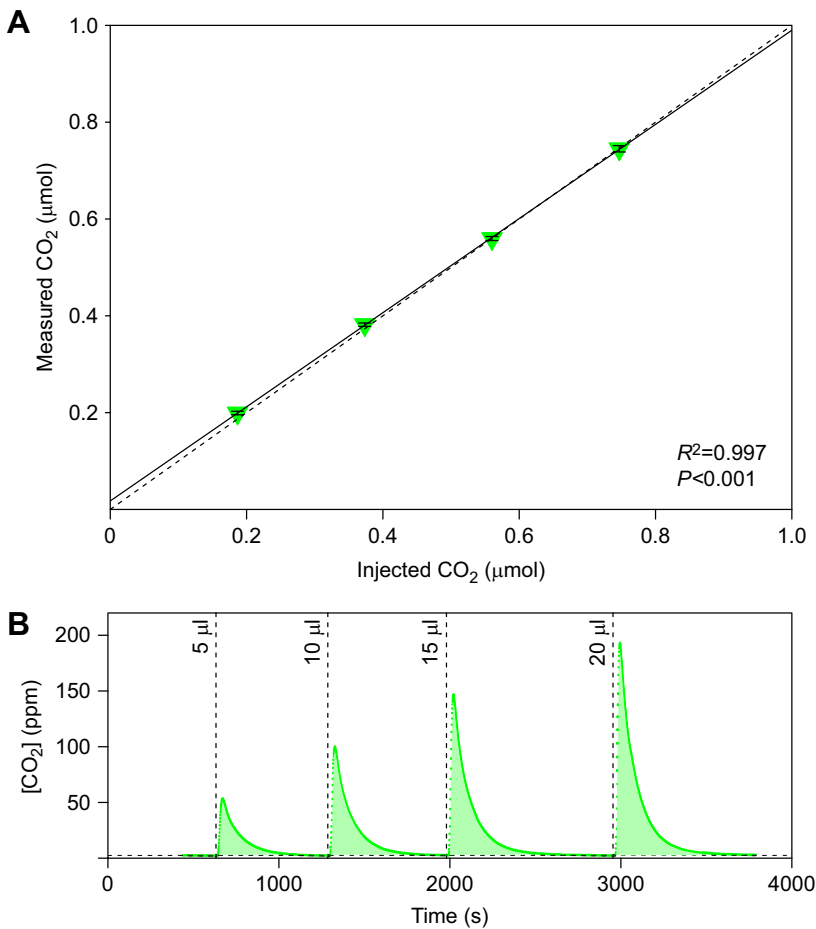


Fig. 2. Series 1, validation of the experimental apparatus.

(A) Measured CO_2 content (μmol) relative to injected CO_2 content (Series 1). Known volumes of CO_2 -saturated water (5, 10, 15 or 20 μl) were injected into the measuring chamber of the apparatus, and CO_2 content was calculated based on the physical solubility of CO_2 in water under the tested conditions (see Fig. 1 for details on the apparatus). Measurements of CO_2 content were carried out with an infrared CO_2 analyser in the gas phase, after diffusion of CO_2 across a hollow fibre membrane. All data are means \pm s.e.m. ($n=6$) and the linear regression was according to: $\text{CO}_2 \text{ measured} = 0.018 \pm 0.005 + 0.972 \pm 0.011 \times (\text{CO}_2 \text{ injected})$. (B) Representative trace of CO_2 concentration ($[\text{CO}_2]$, ppm) measured with an infrared CO_2 analyser. In each trial, four volumes of CO_2 -saturated water were injected into the measuring chamber and injection time points are indicated by vertical dashed lines. Data were analysed by integrating under the $[\text{CO}_2]$ curve (green shading) and subtracting the average baseline reading (horizontal dashed line).

Eqn 2. The integral was taken from the time point at which the peristaltic pump was re-started (t_1) until $[\text{CO}_2]$ returned to baseline (t_2), which was calculated as the average $[\text{CO}_2]$ during continuous \dot{M}_{CO_2} measurements corrected for drift during stop-flow; see Fig. S1B. The obtained CO_2 content was then divided by the length of the stop-flow period (min).

\dot{M}_{O_2} was determined from the slope of the P_{O_2} curve during stop-flow, selecting a 10 min period immediately before re-starting the flow; see Fig. S1A. \dot{M}_{O_2} was then calculated as:

$$\dot{M}_{\text{O}_2} = -\frac{\delta P_{\text{O}_2}}{\delta t} \times \frac{(V_c - V_a)}{1000} \times \alpha_{\text{O}_2} \times 60, \quad (3)$$

where $-(\delta P_{\text{O}_2}/\delta t)$ (mmHg s^{-1}) is the slope of the P_{O_2} curve during stop-flow, V_c and V_a (ml) are the volumes of the chamber and the animal (based on animal wet mass and assuming a density equal to water), respectively, and α_{O_2} ($\mu\text{mol l}^{-1} \text{mmHg}^{-1}$) is the solubility of O_2 in water (Boutilier et al., 1984). A control stop-flow recording was performed without an animal and the obtained P_{O_2} slope was subtracted from every animal recording (on average, control P_{O_2} slope was $14 \pm 3\%$ of animal respiration slopes). Respiratory exchange ratio (RER) was calculated as stop-flow \dot{M}_{CO_2} over \dot{M}_{O_2} .

All data were analysed in RStudio v0.98.1049 (Rv3.3.1). Results of linear regression analyses are presented as adjusted R^2 and P -values. Differences in regressions slopes and between \dot{M}_{O_2} and \dot{M}_{CO_2} measurements were compared by ANCOVA with animal mass as a covariate, and RER, pH and P_{O_2} were compared by ANOVA ($P < 0.05$). All data are means \pm s.e.m.

RESULTS AND DISCUSSION

In Series 1, injections of CO_2 -saturated water into the measuring chamber were used to demonstrate the precision and accuracy of the apparatus. After initiating a run, $[\text{CO}_2]$ readings quickly decreased to an average baseline of 2.6 ± 0.1 ppm. Injections of CO_2 were reflected in a peak in $[\text{CO}_2]$ in the gas phase (Fig. 2B) with a time lag of several seconds for the tested gas flow rates. The measured content of CO_2 corresponded well with that injected (Fig. 2A; $R^2 = 0.997$, $P < 0.001$). Thus, injected CO_2 quickly and completely diffused from the water to the gas phase across the HFM.

In Series 2, dragonfly nymphs spanning a wide range of wet masses were used to validate the apparatus for *in vivo* measurements of \dot{M}_{CO_2} and \dot{M}_{O_2} . Few other studies have measured respiratory rates in aeshnid dragonfly nymphs and, to our knowledge, no other study has performed simultaneous measurements of \dot{M}_{CO_2} and \dot{M}_{O_2} . Petitpre and Knight (1970) measured \dot{M}_{O_2} in nymphs of *Anax junius* over a range of animal dry masses. Re-calculating their data (assuming that dry mass is 25% of animal wet mass; Dermott and Paterson, 1974) yielded \dot{M}_{O_2} values ($\mu\text{mol min}^{-1}$) that scaled with wet mass (m) according to:

$$\dot{M}_{\text{O}_2} = 0.100 \pm 0.011 \times m^{0.624 \pm 0.106}, \quad (4)$$

and these results were not significantly different from the data generated in the present study ($P = 0.652$; Fig. S2):

$$\dot{M}_{\text{O}_2} = 0.108 \pm 0.011 \times m^{0.678 \pm 0.038}. \quad (5)$$

In addition, both scaling exponents for \dot{M}_{O_2} are within the range that has been previously reported for invertebrates (Glazier, 2005).

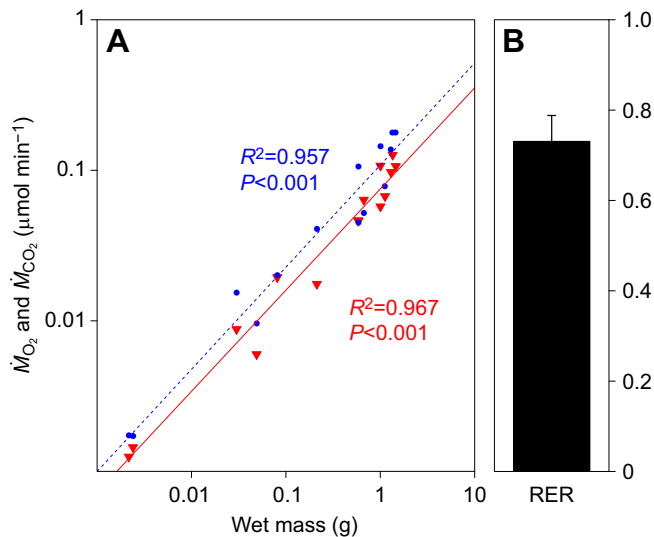


Fig. 3. Series 2, validation of the experimental apparatus for *in vivo* measurements. (A) Rates of CO₂ production (\dot{M}_{CO_2} , $\mu\text{mol min}^{-1}$, red triangles) and O₂ consumption (\dot{M}_{O_2} , blue circles) of aeshnid dragonfly nymphs ($n=15$) as a function of animal wet mass (g) on a double-log scale (Series 2). Data points represent individual measurements and power regression lines are indicated for both parameters, corresponding to the linear models: $\log_{10}(\dot{M}_{\text{CO}_2}) = -1.124 \pm 0.038 + 0.672 \pm 0.033 \log_{10}(m)$ ($R^2=0.967$, $P<0.001$) and $\log_{10}(\dot{M}_{\text{O}_2}) = -0.965 \pm 0.044 + 0.678 \pm 0.038 \log_{10}(m)$ ($R^2=0.957$, $P<0.001$). The slopes for both parameters were significantly different (ANCOVA, $P=0.015$). (B) Average respiratory exchange ratio (RER) calculated from the individual data in A, as $\dot{M}_{\text{CO}_2}/\dot{M}_{\text{O}_2}$. Data are means \pm s.e.m.

Therefore, \dot{M}_{O_2} can be viewed as a reliable internal reference for the validation of the novel \dot{M}_{CO_2} measurements.

Continuous measurements of \dot{M}_{CO_2} , before and after stop-flow, were not significantly different ($P=0.273$) and averaged over all animals $0.070 \pm 0.017 \mu\text{mol min}^{-1}$. Stop-flow \dot{M}_{CO_2} was significantly lower than continuous \dot{M}_{CO_2} ($P=0.014$) and was on average $0.051 \pm 0.011 \mu\text{mol min}^{-1}$ (Fig. S3). This discrepancy was driven entirely by the largest individuals measured ($m > 1100$ mg, $n=4$), where \dot{M}_{CO_2} was lower during stop-flow compared with continuous readings, and in a subset of data excluding these individuals there was no significant difference between continuous and stop-flow measurements of \dot{M}_{CO_2} ($P=0.176$, $n=11$). This is an important result and indicates that there is no methodological discrepancy between the two measurements, and \dot{M}_{CO_2} can be determined reliably using the continuous and stop-flow approaches.

The observed discrepancy between \dot{M}_{CO_2} measurements in the largest individuals may be the result of: (1) CO₂ loss to the environment during stop-flow; (2) formation of HCO₃⁻ during stop-flow and its retention during washout; or (3) a lower animal \dot{M}_{CO_2} during stop-flow. Loss of CO₂ from the system seems unlikely, as CO₂ injected in Series 1 was recovered entirely across the HFM, using peak [CO₂] values that were in line with those produced by the animal. Likewise, CO₂ retained in the system as HCO₃⁻ should be reflected in a lower pH and a higher \dot{M}_{CO_2} in the continuous animal recording after stop-flow (phase v), compared with the initial recording (phase ii), neither of which was observed (in the whole dataset or in the subset of largest individuals; Figs S3, S4). Thus it seems possible that \dot{M}_{CO_2} in the largest individuals was lower during stop-flow periods because of a reduction in metabolic rate, perhaps related to the accumulation of metabolites in the water, decreasing pH and P_{O_2} .

Fig. 3A depicts stop-flow \dot{M}_{CO_2} data in direct comparison with the control measurements of \dot{M}_{O_2} taken over the same stop-flow period; \dot{M}_{CO_2} scaled with wet mass according to:

$$\dot{M}_{\text{CO}_2} = 0.075 \pm 0.007 \times m^{0.672 \pm 0.033}. \quad (6)$$

These results lend further support to the validity of stop-flow \dot{M}_{CO_2} measurements, which corresponded well with the previously validated \dot{M}_{O_2} data, producing physiologically relevant RER (0.73 ± 0.06 ; Fig. 3B), and RER in the subset of the largest individuals was not significantly different from that of all others ($P=0.886$). Thus it appears that the largest individuals had lower stop-flow \dot{M}_{CO_2} as well as \dot{M}_{O_2} , which is in line with a decreased metabolic rate during stop-flow (but not with CO₂ loss to the environment or the retention of HCO₃⁻). Clearly, the effects of changing stop-flow respirometry conditions on the respiratory rates of dragonfly nymphs deserve further attention, especially as these effects may be sensitive to animal life stage.

The range of animal sizes investigated here spans nearly the entire aquatic life stage of aeshnid dragonflies and a 700-fold increase in body mass. The two smallest individuals were hatched in the laboratory, and both were third instar nymphs when measured (2.17 and 2.40 mg wet mass). Even for these small animals, the CO₂ signal after stop-flow (duration 125 and 71 min) was on average 17 ± 3 -fold larger than baseline readings. Therefore, it appears feasible to measure \dot{M}_{CO_2} in animals that are yet another order of magnitude smaller. Finally, because the water phase is in constant contact with the CO₂-free (but normoxic) purge-gas across the HFM, long-term experiments are possible without the animal depleting O₂ in the system (Fig. S4). Likewise, gas tensions in the measuring chamber can be easily controlled by changing the composition of the purge-gas, presenting great potential for hypoxia studies. The described apparatus is scalable, and thus a wide range of aquatic species may be studied, from invertebrates to larval and juvenile vertebrates such as fish and amphibians.

Acknowledgements

Thanks are due to Mike Sackville and Alexander Cheng for their help with animal capture and care.

Competing interests

The authors declare no competing or financial interests.

Author contributions

T.S.H. and P.G.D.M. conceived the study. T.S.H. built the apparatus, performed the experiments and wrote the manuscript. All authors participated in the analysis and interpretation of the data and revised the manuscript.

Funding

This study was supported by Natural Sciences and Engineering Research Council of Canada (NSERC) Accelerator [462242-2014 to P.M.; 446005-13 to C.J.B.] and Discovery Grants [2014-05794 to P.G.D.M.; 261924-13 to C.J.B.] and a Canada Foundation for Innovation (CFI) John R. Evans Leaders Fund grant [JELF 33979 to P.G.D.M.]

Supplementary information

Supplementary information available online at <http://jeb.biologists.org/lookup/doi/10.1242/jeb.150235.supplemental>

References

- Arazawa, D. T., Oh, H.-I., Ye, S.-H., Johnson, C. A., Jr, Woolley, J. R., Wagner, W. R. and Federspiel, W. J. (2012). Immobilized carbonic anhydrase on hollow fiber membranes accelerates CO₂ removal from blood. *J. Membr. Sci.* **403**, 25–31.
- Boutlier, R. G., Heming, T. A. and Iwama, G. K. (1984). Physicochemical parameters for use in fish respiratory physiology. In *Fish Physiology*, Vol. XA (ed. W. S. Hoar and D. J. Randall), pp. 403–426. New York: Academic Press.

- Dean, J. A.** (1999). *Lange's Handbook of Chemistry*. New York: Mc Graw Hill Book Company.
- Dermott, R. M. and Paterson, C. G.** (1974). Determining dry weight and percentage dry matter of chironomid larvae. *Can. J. Zool.* **52**, 1243-1250.
- Glazier, D. S.** (2005). Beyond the '3/4-power law': variation in the intra- and interspecific scaling of metabolic rate in animals. *Biol. Rev.* **80**, 611-662.
- Kaar, J. L., Oh, H.-I., Russell, A. J. and Federspiel, W. J.** (2007). Towards improved artificial lungs through biocatalysis. *Biomaterials* **28**, 3131-3139.
- Nolan, H., Wang, D. and Zwischenberger, J. B.** (2011). Artificial lung basics: fundamental challenges, alternative designs and future innovations. *Organogenesis* **7**, 23-27.
- Petitpre, M. F. and Knight, A. W.** (1970). Oxygen consumption of the dragonfly, *Anax junius*. *J. Insect Physiol.* **16**, 449-459.
- Pfeiffer, T. J., Summerfelt, S. T. and Watten, B. J.** (2011). Comparative performance of CO₂ measuring methods: Marine aquaculture recirculation system application. *Aquacult. Eng.* **44**, 1-9.
- Potkay, J. A.** (2014). The promise of microfluidic artificial lungs. *Lab. Chip.* **14**, 4122-4138.
- Stiller, K. T., Moran, D., Vanselow, K. H., Marxen, K., Wuertz, S. and Schulz, C.** (2013). A novel respirometer for online detection of metabolites in aquaculture research: evaluation and first applications. *Aquacult. Eng.* **55**, 23-31.
- Strueber, M.** (2015). Artificial lungs: are we there yet? *Thorac. Surg. Clin.* **25**, 107-113.